Role of the basic character of α-sarcin's NH_2-terminal β-hairpin in ribosome recognition and phospholipid interaction.

Elisa Álvarez-García, Álvaro Martínez-del-Pozo* and José G. Gavilanes*.

Departamento de Bioquímica y Biología Molecular I, Facultad de Ciencias Químicas, Universidad Complutense, 28040 Madrid, Spain.

*Corresponding authors: Tel: 34 91 394 4259. Fax: 34 91 394 4159. E-mail addresses: alvaro@bbm1.ucm.es (AMP) and ppgf@bbm1.ucm.es (JGG).

Short title: Role of β-hairpin positive charges in ribotoxins' function.

Abstract

Ribotoxins are a family of toxic extracellular fungal RNases that first enter into the cells and then exert a highly specific ribonucleolytic activity on the larger rRNA molecule, leading to protein synthesis inhibition and cell death by apoptosis. α-Sarcin is the best characterized ribotoxin. Previous characterization of a deletion variant of this protein showed that its long NH_2-terminal β-hairpin is essential for its cytotoxicity. Docking, enzymatic, and lipid-protein interaction studies suggested that this β-hairpin establishes specific interactions with ribosomal proteins and that it is a region involved in the interaction with cell membranes. Consequently, in order to assess the influence of the basic character of this NH_2-terminal β-hairpin (there are 1 arginine and 4 lysines along its 16 residues) on the ribotoxins cytotoxic ability, five individual mutants substituting these 5 basic residues by glutamic acid were produced, purified to homogeneity, and characterized. Regarding ribosomal recognition, all mutants showed a diminished activity in a cell-free reticulocyte lysate, whereas the activity against an oligoribonucleotide mimicking the sarcin/ricin loop rRNA (SRL) or the homopolymer poly(A) remained unaffected, confirming that the mutated basic residues participate in electrostatic interactions with other ribosomal elements apart from this SRL. The study of the interaction with phospholipid vesicles showed that Lys 17, Arg 22, and, most importantly, Lys 14 and Lys 21, are crucial residues in the first stages of the aggregation phenomenon, where protein-vesicle and protein-protein interactions are required. The data obtained reveal that electrostatic interactions involving basic residues of the β-hairpin are required not only for establishing specific interactions with ribosomal regions other than the SRL but also to explain the ability of the protein to interact with acid phospholipid bilayers.

Keywords: ribotoxin, protein-lipid interaction, ribosome recognition, restrictocin, electrostatic interaction, ribonuclease, site-directed mutagenesis

Introduction

α-Sarcin is the most representative member of ribotoxins, a family of fungal natural killers characterized by their exquisite ribonucleolytic specificity against ribosomes and their ability to cross cellular membranes in the absence of any known protein receptor [1,2]. These toxic proteins cleave just a single phosphodiester bond of the large rRNA fragment, located at an evolutionarily conserved loop with important roles in ribosome function [3-5]. This cleavage inhibits protein biosynthesis, leading to cell death by apoptosis [6]. This important region has become to be known as the sarcin/ricin loop (SRL) because it is not only the target of α-sarcin and the rest of ribotoxins but also of the much larger group of plant ribosome-inactivating proteins (RIP), best represented by ricin [7,8].

Most ribotoxins show a high degree of sequence identity [9-12] that is also manifested in the three-dimensional structure of the two only ribotoxins studied at this level, restrictocin [13,14] and α-sarcin [15-18]. Both proteins fold into an α+β structure with a central five-stranded antiparallel β-sheet and an α-helix of almost three turns and display long and unstructured loops (Fig.1) [15,19,20]. Residues 1–26 form a long NH_2-terminal β-hairpin that can be considered as two consecutive minor β-hairpins connected by a hinge region with its most distal part jutting out as a solvent exposed protuberance (Fig. 1). This β-hairpin is one of the regions showing the highest sequence variability among ribotoxins [9-12,21]. An α-sarcin mutant involving the deletion of this protuberance, α-sarcin Δ(7–22), retained the same conformation as the wild-type protein, as ascertained from its three-dimensional structure in solution [22]. However, functional and enzymatic studies revealed that this mutant exhibited ribonuclease activity against naked rRNA and synthetic substrates but lacked the ability to specifically cleave the SRL in intact ribosomes [23]. These results were explained by *in silico* studies that predicted how this NH_2-terminal β-hairpin could establish essential interactions, mostly of electrostatic nature, with

specific ribosomal proteins in order to direct the ribotoxin to the SRL region of the ribosome [18].

In addition to their specific and lethal ribonucleolytic activity, ribotoxins can also cross phospholipid membranes due to their ability to interact with acid phospholipid-containing bilayers [6,24-28]. This is the basis to explain why they are especially active on transformed or virus-infected cells [6,29,30], although any ribosome could be potentially inactivated by them, given the universal conservativeness of the SRL. According to the current model accepted to explain the ability of α-sarcin to interact with phospholipid bilayers, the protein would be initially adsorbed to the charged polar head groups of the phospholipids, and then would partially penetrate the interface of the bilayer to interact with a portion of the lipid hydrocarbon chains [1,6,26,31,32]. This intercalation within the lipid matrix would promote fusion and permeability changes in the bilayers, processes that would presumably be involved in the passage of the protein across the membrane of its target cells. Two regions of the protein, located at opposite ends of the protein molecule, have been proposed to be specifically involved in vesicle aggregation [33]. These regions would be loop 2 and, again, the NH_2-terminal β-hairpin (Fig. 1), which consequently would also participate in the interaction with cell membranes. In good accordance with this proposal, the α-sarcin Δ(7–22) mutant also displayed a diminished ability to interact with phospholipid lipid vesicles showing a behavior compatible with the absence of one vesicle-interacting region [23]. In agreement with all these conclusions, the deletion mutant exhibited a very low cytotoxicity on human rhabdomyosarcoma cells [23].

α-Sarcin is a highly charged protein, with a high isoelectric point [34;,35]. This high content of positively charged residues, mostly located at the loops and the NH_2-terminal β-hairpin, is probably required for recognizing and binding not only to its highly negatively charged target, the SRL rRNA, but also to ribosomal proteins and cellular membranes [18,36, 37]. In this context, the role of the positively charged residues located at the NH_2-terminal β-hairpin (Table 1) in these different but closely related events has been studied in the work herein presented.

Materials and methods

DNA manipulations

All materials and reagents were of molecular biology grade. Cloning procedures, oligonucleotide site-directed mutagenesis, and bacterial manipulations were carried out as previously described [28,38,39]. The mutagenic primers used to substitute the mutated residues are shown in Table 1. Presence of only the mutation expected in each case was confirmed by sequencing the complete cloned cDNA. The plasmid used as the template for mutagenesis experiments, containing the cDNA sequence coding for wild-type α-sarcin, has already been described [38,40].

Protein production and purification

E. coli BL21 (DE3) cells cotransformed with a thioredoxin-producing plasmid (pT-Trx) and the corresponding α-sarcin mutant plasmids were used to produce the different proteins studied, as previously described [38,40,41]. Fungal wild-type α-sarcin was obtained as previously reported [28]. Protein purification included ion exchange and molecular exclusion chromatographies [28]. PAGE of proteins, Western blot immunodetection, protein hydrolysis, and amino acid analysis were performed according to standard procedures [38,41].

Spectroscopic characterization

Absorbance measurements were performed on an Beckman DU640 spectrophotometer at room temperature in cells with a 1 cm optical path length at a scanning speed of 240 nm/min. Circular dichroism (CD) spectra were obtained on a Jasco 715 spectropolarimeter, equipped with a thermostated cell holder and a NesLab-111 circulating water bath, at 0.2 nm/s. The instrument was calibrated with (+)-10-camphorsulfonic acid. CD spectra were recorded in

cylindrical cells with an optical path length of 0.1 and 1.0 cm. Mean residue weight ellipticity is expressed in units of deg cm^2 $dmol^{-1}$. Thermal denaturation profiles were obtained by measuring the temperature dependence of the ellipticity at 220 nm in the range 25–80ºC; the temperature was continuously changed at a rate of 0.5ºC/min. Fluorescence emission spectra were recorded on an SLM Aminco 8000 spectrofluorimeter at 25ºC using a slit width of 4 nm for both excitation and emission beams. The spectra were recorded for excitation at 275 and 295 nm and both were normalized by considering that Tyr emission above 380 nm is negligible. The Tyr contribution was calculated as the difference between the two normalized spectra. Thermostated cells with a path length of 0.2 and 1.0 cm for the excitation and emission beams, respectively, were used. The temperature was controlled using a circulating water bath. All these experiments were made with the proteins dissolved in 50 mM sodium phosphate, pH 7.0, containing 0.1 M NaCl following procedures described before [28,38].

Ribonucleolytic activity

The ribonucleolytic activity of α-sarcin on eukaryotic ribosomes was followed by detecting the release of the near 400-nts α-fragment from a rabbit cell-free reticulocyte lysate. Production of this fragment was visualized by ethidium bromide staining after electrophoresis on denaturing 2.4% agarose gels. The specific cleavage by α-sarcin of an SRL-like synthetic 35-mer RNA was also studied. The synthesis of this SRL RNA was carried out as described [42]. The assay was performed with 4 μM SRL RNA and incubation for 15 min at 37ºC in 50 mM Tris-HCl buffer, pH 7.0, containing 0.1 M NaCl and 5 mM EDTA. The reaction products were detected by ethidium bromide staining after electrophoretic separation on a denaturing 19% (w/v) polyacrylamide gel. The specific action of α-sarcin produced 21- and 14-mer fragments. In addition, the activity of the purified proteins against homopolynucleotides (zymogram) was also assayed. Volumograms of the electrophoretic bands (based on integrating all of the pixel intensities comprising each spot) were obtained with the UVI-Tec

photo documentation system and UVIsoft UVI band Windows Application V97.04. These data were used to quantify the enzyme activity in the different assays. All these enzymatic assays were performed as previously described [28,38,42]. Convenient controls were routinely performed to test potential non-specific degradation of the substrates, which did not occur under the conditions used.

Phospholipid vesicle aggregation

Dimyristoylphosphatidylglycerol (DMPG) was purchased from Avanti Polar Lipids Inc. (Alabaster, USA). Vesicles were formed by hydrating a dry lipid film with 15 mM Tris, pH 7.0 containing 0.1 M NaCl and 1 mM EDTA for 60 min at 37ºC. This lipid suspension was then subjected to five cycles of extrusion through two stacked 0.1-mm (pore diameter) polycarbonate membranes [33]. The average diameter of the vesicle population was 100 nm (85% of the vesicles in the range 75–125 nm), as determined by electron microscopy studies [33]. Aggregation was monitored as previously described [24,28] by measuring the increase in absorbance at 400 nm of a suspension of vesicles (30 mM final lipid concentration) after addition of a small aliquot of a freshly prepared solution of protein.

Results

Protein purification and structural characterization

All six proteins, wild-type and the five single mutants, were purified to homogeneity and in milligram amounts (Table 2), according to their SDS-PAGE behavior (Fig. 2A) and amino acid composition. This composition was consistent with the mutations expected in each case. All them were also detected by a rabbit anti-α-sarcin serum in Western blot assays (Fig. 2B). The amino acid analysis and the corresponding UV-absorbance spectra were used to calculate their extinction coefficients (Table 2).

The native conformation of the wild-type protein was fully preserved in all the mutants, according to the coincidence of their far-UV circular dichroism spectra (Fig. 3A). The spectral features in the near-UV range (Fig. 3B) were also very similar with just the mutants showing small differences practically within the error range of this type of determination. Accordingly, fluorescence emission spectra for both wild-type and the five mutant proteins were also very similar (Fig. 4 and Table 2). These results again suggested that the wild-type protein conformation was retained in the mutants.

All mutants studied showed a slightly decreased conformational stability in comparison with the wild-type protein (Fig. 5) according to their T_m values and the corresponding estimated Δ(ΔG) (Table 3). Apparently, substitution of Lys 21 rendered the most unstable mutant. However, the obtained low Δ(ΔG) values and the shape of the thermal denaturation profiles (Fig. 5) were also in agreement with the assumption that the mutant proteins displayed an overall conformation very similar to that of wild-type α-sarcin.

Enzymatic characterization

All mutants studied displayed a slightly lower specific ribonucleolytic activity than wild type α-sarcin when assayed against intact ribosomes in a rabbit reticulocyte lysate (Fig. 6). However, all them behaved indistinguishable when assayed against less specific substrates such as an SRL-like oligonucleotide (Fig.7) or the hompolynucleotide poly(A) (Fig. 8). Unexpectedly, the α-sarcin K14E mutant was also able to cleave poly(C), an homopolynucleotide resistant to the action of the wild-type protein or the other mutants here studied (Fig. 8).

Interaction with Phospholipid Vesicles

In the present study the aggregation of DMPG vesicles promoted by the wild-type protein and the NH_2-terminal β-hairpin mutants was followed by recording the increase of the apparent absorbance at 400 nm of a suspension

of DMPG vesicles after addition of a small aliquot of a freshly prepared protein (Fig. 9). The kinetic profiles of this phospholipid vesicles aggregation showed a biphasic behavior (Fig. 9) that was only observed at very low protein/lipid molar ratios for the wild-type α-sarcin and the K11E mutant, as expected from previous studies [33]. On the other hand, the other four mutants studied displayed a much different kinetic pattern of vesicle aggregation being the biphasic pattern much more evident, even at high protein/lipid molar ratios (Fig. 9). These differences were especially significant for mutants K14E and K21E. Apparently, the first aggregation step would be the one being more affected by the mutations, as revealed by the net apparent absorbance change observed at shorted times (Fig. 10). Simultaneously, a delay in the onset of the formation of the structures appearing at longer times was also observed for mutants K14E, K21E, and R22E (Fig. 9), being again much more pronounced at the lower protein concentrations used.

Discussion

The SRL sequence and conformation is maintained in all ribosomes known so far. Furthermore, structural characterization of different SRL-like oligoribonucleotides has revealed how these isolated structures adopt the same conformation as well [43-45], being indeed susceptible of specific recognition and cleavage by ribotoxins [42,46]. The toxin and SRL structural determinants involved in their mutual recognition have been identified and characterized [13-15,47]. However, this cleavage reaction against an isolated SRL-like RNA takes place at rates about 1000-fold slower than when using intact ribosomes [37,46] indicating that additional recognition elements are needed for the optimal ribotoxins' inactivation action against ribosomes. The involvement of the ribosomal context in terms of electrostatic interactions has been suggested not only to justify this recognition and binding enhancement but also to explain the differences found when these toxins are assayed against ribosomes of different origins [18,37]. Electrostatic interactions involving the α-sarcin NH_2-terminal-β-hairpin have been also suggested to mediate α-sarcin specific recognition of

ribosomal proteins [18]. In fact, mutation of some basic residues that lie outside the restrictocin-SRL interface has been shown to decrease markedly the ribosomes cleaving rates without having any effect on the kinetics of assays employing an isolated SRL-like oligoribonucleotide [37]. It is also well proven how electrostatic interactions are needed for the establishment of the associations needed to allow the passage of ribotoxins across acid phospholipid membranes [24,25,27] and the α-sarcin NH_2-terminal-β-hairpin is one of the protein regions that has been involved in this membrane recognition mechanism [23,48].

Ribotoxins are basic proteins with high pI values [1] due to their high content of basic residues mostly located at their unstructured loops [13-15]. Five of them concentrate at the α-sarcin NH_2-terminal-β-hairpin being indeed residues 14, 17, 21, and 22 conserved among the different ribotoxins known, with the exception of hirsutellin A, a much smaller ribotoxin of recent characterization [12]. Therefore, with the aim of defining the role of electrostatic interactions involving α-sarcin NH_2-terminal-β-hairpin, these five basic amino acid residues were mutated to Glu and their involvement in the molecular mechanism of α-sarcin cytotoxicity was studied.

Structural characterization of the isolated purified proteins revealed that all retained the wild-type conformation, as indicated by their spectroscopic and thermodynamical characterization. Only minor changes were observed after inspection of the near-UV CD (Fig. 3) and fluorescence emission spectra (Fig. 4), most probably due to the presence of Tyr 18 and 25 and Trp-4, a residue that dominates α-sarcin emission [49], within the sequence of the mutated NH_2-terminal-β-hairpin. All mutants were slightly less stable than the wild-type protein (Table 3) but the differences were even smaller than those ones found among the different natural ribotoxins known [12,48], in good agreement with previous results indicating that the NH_2-terminal-β-hairpin folds as a rather independent structure with low influence on the global thermostability of the protein [23]. This observation is in good accordance with the fact that most of the residues mutated do not establish obvious interactions with any other amino acid of the protein globular core with perhaps the only exception of the non-

conserved Lys 11 [15]. The highest difference was found for α-sarcin K21E, being the mutated Lys a residue involved in an electrostatic interaction with Glu-19 [50], an interaction which is not possible for the mutant protein.

Regarding their enzymatic characterization, it seems clear from the results presented that any charge reversion at the NH_2-terminal-β-hairpin results in a diminished specific activity against intact ribosomes (Fig. 6) without affecting the less specific ribonucleolytic action of the protein (Fig. 7 and 8). Lys 11 and 14 had been predicted before to establish electrostatic interactions with specific negative residues from ribosomal proteins [18]. The present results would not only confirm this prediction but also suggest that additional interactions are established between the positively charged side-chains at the NH_2-terminal-β-hairpin and negatively charged ribosomal elements, not only proteins but most probably also rRNA included. The observation of the different specificity displayed by mutant K14E against homopolynucleotides (Fig. 8) reveals that the β-hairpin is also involved in their recognition. This involvement might be in terms of a direct interaction with the polymer or most probably due to a modification of the active site accessibility, as has been also suggested before [15,51]. In fact, these solvent accessibility changes were detected before upon deletion of the β-hairpin [22].

It is well known how α-sarcin interacts with lipid vesicles through electrostatic and hydrophobic interactions promoting events of vesicle aggregation that are followed by lipid mixing occurring between the bilayers of the aggregated vesicles, as would be expected for fusing liposomes [1,24,25,28]. Stopped-flow measurement of the initial rates of this aggregation induced by α-sarcin showed a second-order dependence on phospholipid concentration, suggesting the formation of vesicle dimers as the initial steps of the process [33]. These same experiments revealed that protein-protein interactions were involved in the establishment of the needed contacts to maintain the mentioned vesicle dimers [33]. In the present experiments the use of smaller protein concentrations revealed the existence of a biphasic behavior even at the much longer time scale of minutes used now (Fig. 9). Thus, the first step observed would correspond to the formation of small vesicles aggregates,

mostly stabilized by protein-protein and protein-vesicle interactions, which would later evolve during the second step of the process to much larger structures involving not only aggregation but also fusion events [24,25,33]. This mechanism would be fully compatible with the biphasic behavior observed in these experiments performed at lower protein/lipid molar ratios (Fig. 9) confirming the current model to explain the ability of ribotoxins to cross phospholipid membranes. Furthermore, the mutant showing more similar behavior to the wild-type protein was K11E, a protein where the mutated residue is not conserved among all ribotoxins, suggesting its minor contribution to the passage of the protein across the membranes. On the other hand, all the other four mutants studied showed a delay affecting the onset of the formation of small vesicle aggregates indicating their participation in maintaining the protein-protein and protein-vesicle interactions needed to initiate the aggregation process. The absence of a single positive charge seems to affect dramatically the accepted mechanism being this effect stronger for replacement of Lys residues 14 and 21. In fact, mutation of these two residues even impairs the formation of the larger aggregates according to the delay also observed for the second stage of the aggregation process. A similar behavior for the myelin basic protein has been attributed to the instability of the protein-protein interactions needed to aggregate the vesicles and most probably this would also be the case for these mutants. Overall, the lipid-protein interaction characterization suggest that residues Lys 14, Lys 17, Lys 21, and Arg 22 do participate directly in the first stages of the vesicle aggregation induced by α-sarcin being much more determinant the role played by residues 14 and 21.

In summary, the result presented show that electrostatic interactions established by the conserved positively charged residues of the α-sarcin NH_2-terminal-β-hairpin are essential not only for the correct specific recognition of the ribosome but also for the optimal establishment of the phospholipid interactions needed to cross the membranes of its presumed target cells.

Acknowledgements

This work was supported by grant BFU2006-04404 from the Ministerio de Educación y Ciencia (Spain). E. A.-G. is recipient of a fellowship from the Ministerio de Educación y Ciencia (Spain).

References

[1] J. Lacadena, E. Álvarez-García, N. Carreras-Sangrà, E. Herrero-Galán, J. Alegre-Cebollada, L. García-Ortega, M. Oñaderra, J.G. Gavilanes, A. Martínez-del-Pozo, FEMS Microbiol. Rev. 31 (2007) 212-237.

[2] N. Carreras-Sangrà, E. Álvarez-García, E. Herrero-Galán, J. Tomé, J. Lacadena, J. Alegre-Cebollada, M. Oñaderra, J.G. Gavilanes and A. Martínez-del-Pozo, Cur. Pharm. Biotechnol. 9 (2008) 153-160.

[3] D.G. Schindler, J.E. Davies, Nucleic Acids Res. 4 (1977) 1097–1110.

[4] Y.L. Chan, Y. Endo, I.G. Wool, J. Biol. Chem. 258 (1983) 12768-12770.

[5] Y. Endo, I.G. Wool, J. Biol. Chem. 257 (1982) 9054–9060.

[6] N. Olmo, J. Turnay, G. González de Buitrago, I. López de Silanes, J.G. Gavilanes, M.A. Lizarbe, Eur. J. Biochem. 268 (2001) 2113–2123.

[7] K. Nielsen, R.S. Boston, Annu. Rev. Plant Physiol. Plant Mol. Biol. 52 (2001) 785–816.

[8] W.J. Peumans, Q. Hao, E.J. Van Damme, FASEB J. 15 (2001) 1493–1506.

[9] J. Wirth, A. Martínez-del-Pozo, J.M. Mancheño, A. Martínez-Ruiz, J. Lacadena, M. Oñaderra, J.G. Gavilanes, Arch. Biochem. Biophys. 343 (1997) 188–193.

[10] A. Martínez-Ruiz, A. Martínez-del-Pozo, J. Lacadena, M. Oñaderra, J.G. Gavilanes, J. Invertebr. Pathol. 74 (1999) 96–97.

[11] A. Martínez-Ruiz, R. Kao, J. Davies, A. Martínez-del-Pozo, Toxicon 37 (1999) 1549–1563.

[12] E. Herrero-Galán, J. Lacadena, A. Martínez-del-Pozo, D.G. Boucias, N. Olmo, M. Oñaderra, J.G. Gavilanes, Proteins 72 (2008) 217–228.

[13] X. Yang, K. Moffat, Structure 4 (1996) 837–852.

[14] X. Yang, T. Gerczei, L.T. Glover, C.C. Correll, Nat. Struct. Biol. 8 (2001) 968–973.

[15] J.M. Pérez-Cañadillas, J. Santoro, R. Campos-Olivas, J. Lacadena, A. Martínez-del-Pozo, J.G. Gavilanes, M. Rico, M. Bruix, J. Mol. Biol. 299 (2000) 1061–1073.

[16] J.M. Pérez-Cañadillas, M. Guenneugues, R. Campos-Olivas, J. Santoro, A. Martínez-del-Pozo, J.G. Gavilanes, M. Rico, M. Bruix, J. Biomol. NMR 24 (2002) 301–316.

[17] M.F. García-Mayoral, D. Pantoja-Uceda, J. Santoro, A. Martínez-del-Pozo, J.G. Gavilanes, M. Rico, M. Bruix, Eur. Biophys. J. 34 (2005) 1057–1065.

[18] M.F. García-Mayoral, L. García-Ortega, E. Álvarez-García, M. Bruix, J.G. Gavilanes, A. Martínez-del-Pozo, FEBS Lett. 579 (2005) 6859–6864.

[19] R. Campos-Olivas, M. Bruix, J. Santoro, A. Martínez-del-Pozo, J. Lacadena, J.G. Gavilanes, M. Rico, Protein Sci. 5 (1996) 969–972.

[20] R. Campos-Olivas, M. Bruix, J. Santoro, A. Martínez-del-Pozo, J. Lacadena, J.G. Gavilanes, M. Rico, FEBS Lett. 399 (1996) 163–165.

[21] L. García-Ortega, J. Lacadena, M. Villalba, R. Rodríguez, J.F. Crespo, J. Rodríguez, C. Pascual, N. Olmo, M. Oñaderra, A. Martínez-del-Pozo, J.G. Gavilanes, FEBS J. 272 (2005) 2536–2544.

[22] M.F. García-Mayoral, L. García-Ortega, M.P. Lillo, J. Santoro, A. Martínez-del-Pozo, J.G. Gavilanes, M. Rico, M. Bruix, Protein Sci. 13 (2004) 1000–1011.

[23] L. García-Ortega, M. Masip, J.M. Mancheño, M. Oñaderra, M.A. Lizarbe, M.F. García-Mayoral, M. Bruix, A. Martínez-del-Pozo, J.G. Gavilanes, J. Biol. Chem. 277 (2002) 18632–18639.

[24] M. Gasset, A. Martínez-del-Pozo, M. Oñaderra, J.G. Gavilanes, Biochem. J. 258 (1989) 569–575.

[25] M. Gasset, M. Oñaderra, P.G. Thomas, J.G. Gavilanes, Biochem. J. 265 (1990) 815–822.

[26] M. Gasset, J.M. Mancheño, J. Lacadena, J. Turnay, N. Olmo, M.A. Lizarbe, A. Martínez-del-Pozo, M. Oñaderra, J.G. Gavilanes, Curr. Topics Pept. Protein Res. 1 (1994) 99–104.

[27] M. Oñaderra, J.M. Mancheño, M. Gasset, J. Lacadena, G. Schiavo, A. Martínez-del-Pozo, J.G. Gavilanes, Biochem. J. 295 (1993) 221–225.

[28] A. Martínez-Ruiz, L. García-Ortega, R. Kao, J. Lacadena, M. Oñaderra, J.M. Mancheño, J. Davies, A. Martínez-del-Pozo, J.G. Gavilanes, Methods Enzymol. 341 (2001) 335–351.

[29] B.H. Olson, J.C. Jennings, V. Roga, A.J. Junek, D.M.Schuurmans, Appl. Microbiol. 13 (1965) 322–326.

[30] C. Fernández-Puentes, L. Carrasco, Cell 20 (1980) 769–775.

[31] M. Gasset, M. Oñaderra, E. Goormaghtigh, J.G. Gavilanes, Biochim. Biophys. Acta 1080 (1991) 51–58.

[32] M. Gasset, M. Oñaderra, A. Martínez-del-Pozo, G.P. Schiavo, J. Laynez, P. Usobiaga, J.G. Gavilanes, Biochim. Biophys. Acta 1068 (1991) 9–16.

[33] J.M. Mancheño, M. Gasset, J. Lacadena, F. Ramón, A. Martínez-del-Pozo, M. Oñaderra, J.G. Gavilanes, Biophys. J. 67 (1994) 1117–1125.

[34] G. Sacco, K. Drickamer, I.G. Wool, J. Biol. Chem. 258 (1983) 5811–5818.

[35] A. Martínez-del-Pozo, M. Gasset, M. Oñaderra, J.G. Gavilanes, Biochim. Biophys. Acta 953 (1988) 280–288.

[36] M. Masip, J. Lacadena, J.M. Mancheño, M. Oñaderra, A. Martínez-Ruiz, Á. Martínez del Pozo, J.G. Gavilanes. Eur J Biochem. 268 (2001) 6190-6196.

[37] A.V. Korennykh, J.A. Piccirilli, C.C. Correll, Nature Str. Mol. Biol. 13 (2006) 436–443.

[38] J. Lacadena, A. Martínez-del-Pozo, J.L. Barbero, J.M. Mancheño, M. Gasset, M. Oñaderra, C. López-Otín, S. Ortega, J. García, J.G. Gavilanes, Gene 142 (1994) 147–151.

[39] E. Álvarez-García, L. García-Ortega, Y. Verdún, M. Bruix, Á. Martínez del Pozo, J.G. Gavilanes. Biol Chem. 387 (2006) 535-541.

[40] J. Lacadena, A. Martínez-del-Pozo, A. Martínez-Ruiz, J.M. Pérez-Cañadillas, M. Bruix, J.M. Mancheño, M. Oñaderra, J.G. Gavilanes, Proteins 37 (1999) 474–484.

[41] L. García-Ortega, J. Lacadena, V. Lacadena, M. Masip, C. de Antonio, A. Martínez-Ruiz, A. Martínez-del-Pozo, Lett. Appl. Microbiol. 30 (2000) 298–302.

[42] R. Kao, A. Martínez-Ruiz, Á. Martínez del Pozo, R. Crameri, J. Davies. Methods Enzymol. 341 (2001) 324-335.

[43] A.A. Szewczak, P.B. Moore, J. Mol. Biol. 247 (1995) 81–98.

[44] C.C. Correll, A. Munishkin, Y.L. Chan, Z. Ren, I.G. Wool, T.A. Steitz, Proc. Natl. Acad. Sci. U.S.A. 95 (1998) 13436–13441.

[45] C.C. Correll, I.G. Wool, A. Munishkin, J. Mol. Biol. 292 (1999) 275–287.

[46] Y. Endo, Y.L. Chan, A. Lin, K .Tsurugi, I.G. Wool, J. Biol. Chem. 263 (1988) 7917–7920.

[47] C.C. Correll, J. Beneken, M.J. Plantinga, M. Lubber, Y.L. Chan, Nucleic Acids Res. 31 (2003) 6806–6818.

[48] L. García-Ortega, J. Lacadena, J.M. Mancheño, M. Oñaderra, R. Kao, J. Davies, N. Olmo, A. Martínez-del-Pozo, J.G. Gavilanes, Protein Sci. 10 (2001) 1658–1668.

[49] C. De Antonio, A. Martínez-del-Pozo, J.M. Mancheño, M. Oñaderra, J. Lacadena, A. Martínez-Ruiz, J.M. Pérez-Cañadillas, M. Bruix, J.G. Gavilanes, Proteins 41 (2000) 350–361.

[50] M.F. García-Mayoral, J.M. Pérez-Cañadillas, J. Santoro, B. Ibarra-Molero, J.M. Sánchez-Ruiz, J. Lacadena, A. Martínez del Pozo, J.G. Gavilanes, M. Rico, M. Bruix, Biochemistry 42 (2003) 13122-13133.

[51] R. Kao, J. Davies, FEBS Lett. 466 (2000) 87-90.

[52] M. Gasset, J.M. Mancheño, J. Laynez, J. Lacadena, G. Fernández-Ballester, Á. Martinez del Pozo, M. Oñaderra, J.G. Gavilanes. Biochim Biophys Acta. 1252 (1995) 126-134.

[53] W.J. Becktel, J.A. Schellman. Biopolymers. 26 (1987) 1859-1877.

Fig. 1. Diagrams showing the three dimensional structure of α-sarcin (A) and a detail of its NH_2-terminal β-hairpin (B). The different basic residues mutated to Glu are shown.

Fig. 2. Analysis by SDS-PAGE of wild-type (1), K11E (2), K14E (3), K17E (4), K21E (5), and R22E (6) versions of α-sarcin. (A) Coomassie Brilliant Blue staining (0.5 μg of protein/lane). (B) Western blot analysis using an anti-(α-sarcin) polyclonal antibody (0.1 μg of protein/lane).

Fig. 3. Circular dichroism spectra in the far (A) and near (B) UV regions, of wild-type (●), K11E (○), K14E (●), K17E (Δ), K21E (△), and R22E (□) versions of α-sarcin. Mean residue weight ellipticity, θ_{MRW}, is expressed in units of degrees x cm^2 x $dmol^{-1}$.

Fig. 4. Fluorescence emission spectra of wild-type, K11E, K14E, K17E, K21E, and R22E versions of α-sarcin at 0.1 mg/ml protein concentration. Spectra 1 were obtained for excitation at 275 nm. Spectra 2 (tryptophan contribution) were obtained for excitation at 295 nm and normalized at wavelengths above 380 nm. Spectra 3 (tyrosine contribution) were calculated as the difference spectra (spectrum 1 - spectrum 2). Fluorescence emission is expressed as percentage considering the intensity at the wavelength of the emission maximum of the wild-type protein, for excitation at 275 nm, as 100. All of the spectra were recorded at 25 °C and pH 7.0.

Fig. 5. Thermal denaturation profiles of wild-type (●), K11E (○), K14E (●), K17E (Δ), K21E (△), and R22E (□) versions of α-sarcin. The measurements were performed by continuously recording the mean residue weight ellipticity at 220 nm (θ_{MRW}) expressed in units of degrees x cm^2 x $dmol^{-1}$.

Fig. 6. Ribosome-inactivating activity assay of wild-type, K11E, K14E, K17E, K21E, and R22E versions of α-sarcin (Upper pannel). A control in the absence of enzyme is also shown (▬). The highly specific ribonucleolytic activity of the

ribotoxins is shown by the release of the 400-nt α-fragment (arrow) from the 28S rRNA of eukaryotic ribosomes. Bands corresponding to 28S and 18S RNA are also indicated. Cell-free reticulocyte lysates were incubated in the presence of 100 ng of each protein. The reaction mixture was analyzed on 2.4% agarose gels and stained with ethidium bromide. Quantitation of these activities is also shown (lower panel), taking as unit the activity found for the wild-type protein in these conditions.

Fig. 7. Activity assay on the 35mer oligonucleotide mimicking the SRL. This substrate was incubated in presence of wild-type, K11E, K14E, K17E, K21E, and R22E versions of α-sarcin (upper panel). A control in the absence of enzyme is also shown (—). Two arrows indicate the position of the 21mer and 14mer oligonucleotides resulting from the specific cleavage of a single phosphodiester bond. The intact 35-mer oligo is also shown. Quantitation of these activities is also shown (lower panel), taking as unit the activity found for the wild-type protein in these conditions.

Fig. 8. Zymogram assay of the ribonucleolytic activity against poly(A) and poly(C) (upper and lower panels, respectively). These assays were made at pH 7.0 employing 0.75 μg of wild-type, K11E, K14E, K17E, K21E, or R22E versions of α-sarcin. A control in the absence of enzyme is also shown (—).

Fig. 9. Kinetic measurement of the effect of the different α-sarcin versions studied on phospholipid vesicle aggregation. The phospholipid/protein molar ratios employed were: 333 (trace 1), 167 (trace 2), 111 (trace 3), 83 (trace 4), and 67 (trace 6). The concentration of DMPG used in these assays was 100 μM.

Fig. 10. The extent of phospholipid vesicles aggregation after 100s, corresponding to the first step of the process, is represented against the concentration employed of the different α-sarcin variants studied. The concentration of DMPG used in these assays was 100 μM.

Table 1. Mutagenic primers used to construct individual mutant versions of wild-type α-sarcin where the NH_2-terminal β-hairpin basic residues had been substituted by Asp. The bases that change original codon to Asp are underlined.

α-sarcin mutant	oligonucleotide sequence
K11E	5’ ttg aac gac cag gag aac ccc aag acc 3’
K14E	5’ cag aag aac ccc gag acc aac aag tat 3’
K17E	5’ ccc aag acc aac gag tat gag acc aaa 3’
K21E	5’ aag tat gag acc gaa cgc ctc ctc tac 3’
R22E	5’ tat gag acc aaa gag ctc ctc tac aac 3’

Table 2. Purification yields (mg per liter of original broth) and spectroscopic properties of the different proteins studied.

Protein	yield	$E^{0.1\%}$ (280 nm, 1 cm)	Q_{Tyr}[a]	Q_{Trp}[a]
WT	7.0 mg/l[b]	1.34	1.00	1.00
K11E	10.5 mg/l	1.31	1.08	1.09
K14E	17.0 mg/l	1.36	0.92	1.03
K17E	12.5 mg/l	1.36	1.06	1.03
K21E	12.5 mg/l	1.35	1.03	1.06
R22E	12.0 mg/l	1.20	1.03	1.13

[a] Relative quantum yield of Tyr and Trp referred to the values of the wild-type protein.

[b] [41].

Table 3. Thermodynamic parameters of the different mutants studied.

Protein	T_m (ºC)	Δ(ΔG) (Kcal/mol)[a]
WT	52.0	0.00
K11E	47.0	-2.09
K14E	48.1	-1.62
K17E	48.1	-1.62
K21E	40.9	-4.64
R22E	47.3	-1.97

[a]$\Delta(\Delta G) = (\Delta H \times \Delta T_m/T_m)$ is the stability change produced by the mutation [ΔH, enthalpy change for the wild-type protein (136 Kcal/mol) determined at pH 7.0 from differential scanning calorimetric measurements [52]; $\Delta Tm = T_m$ (mutant) − T_m (wild-type); T_m, value obtained for the mutant variant] [53].

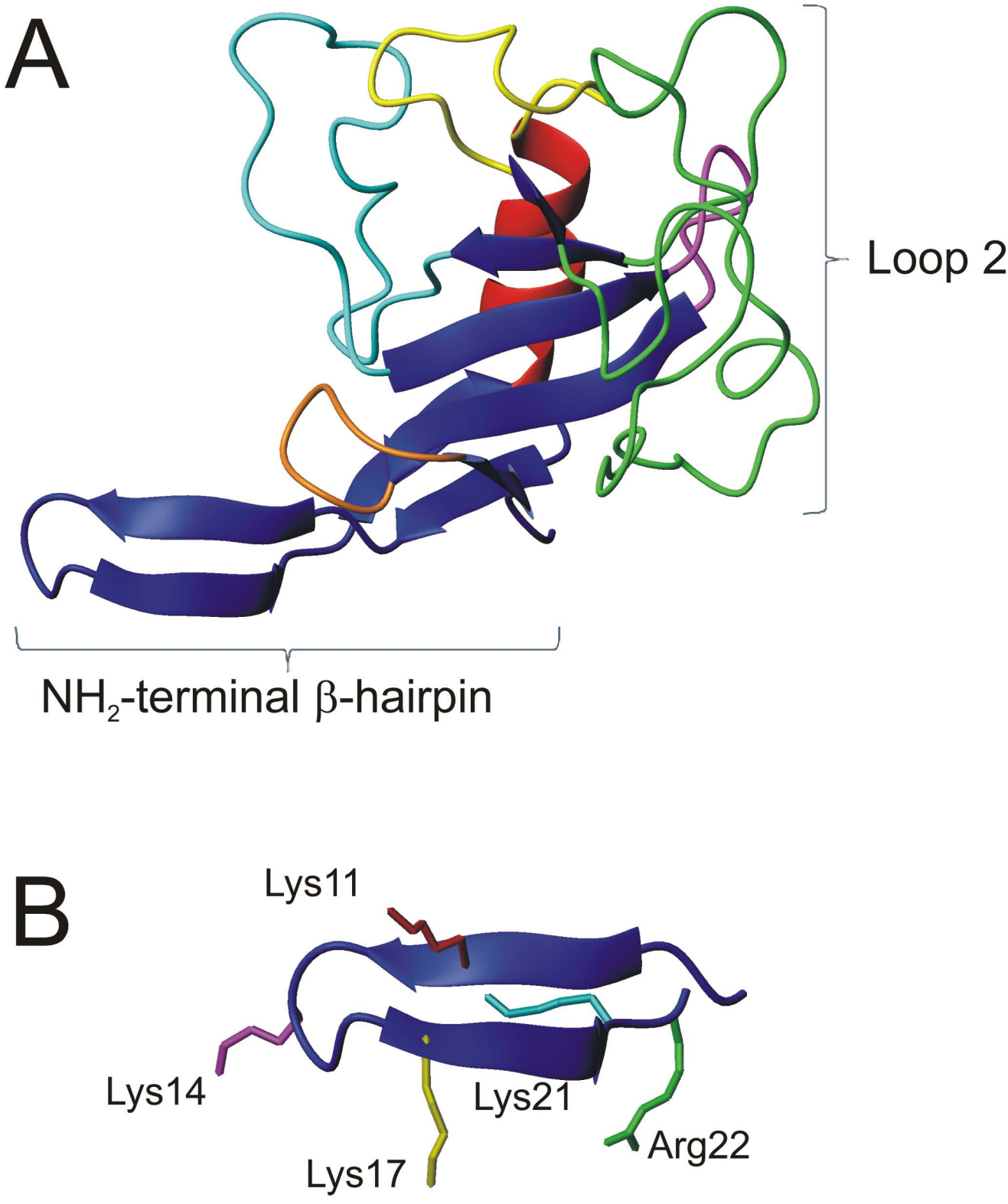
A
Loop 2
NH2-terminal β-hairpin
B
Lys11
Lys14
Lys21
Arg22
Lys17

Figure 1

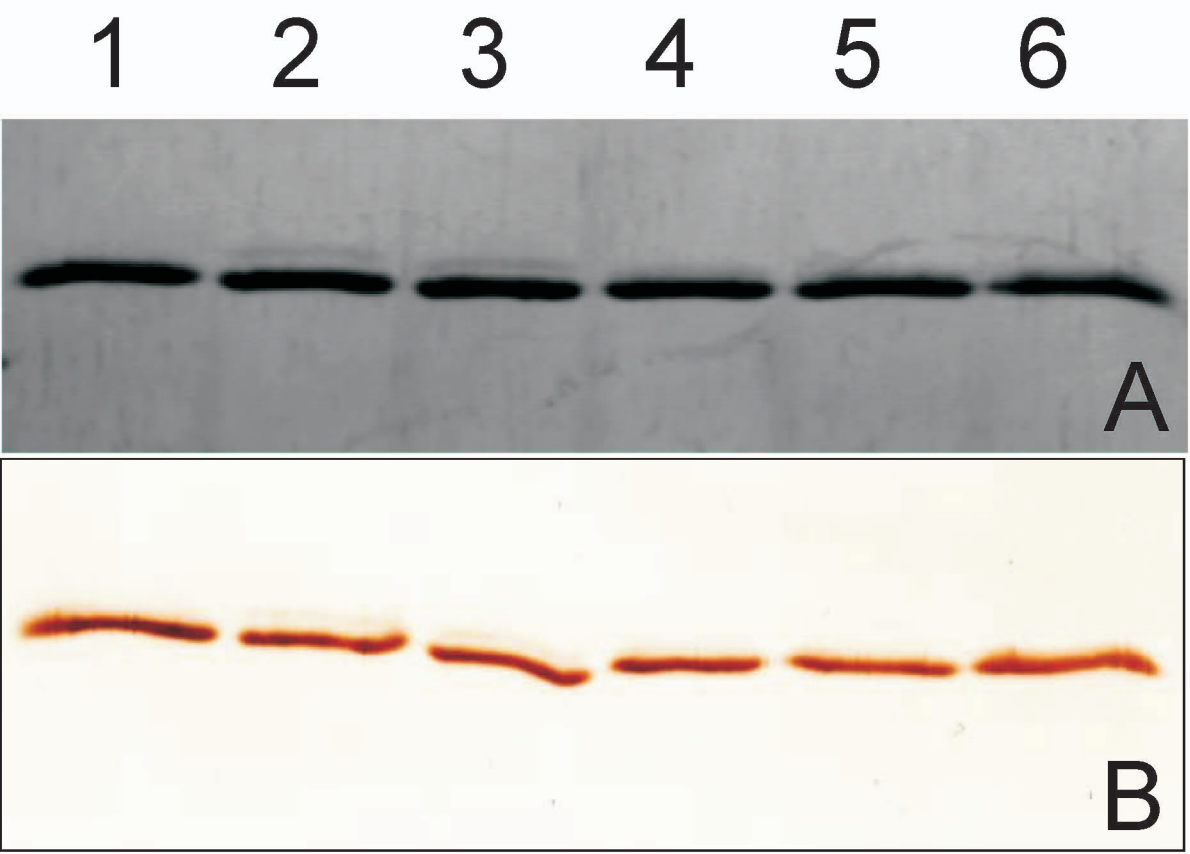

Figure 2

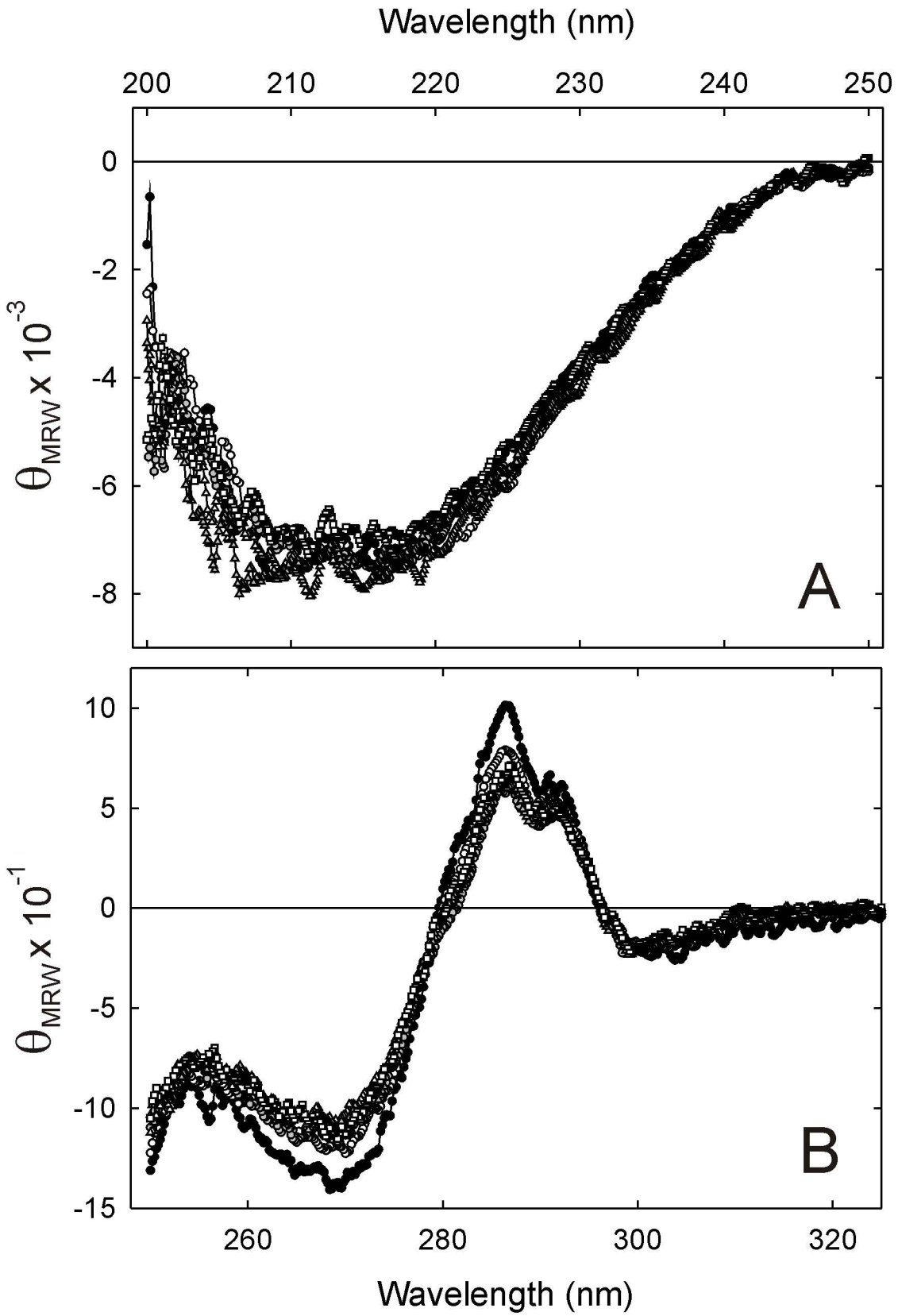
Wavelength (nm)
200
210
220
230
240
250
0
-2
-4
-6
-8
$\theta_{MRW} \times 10^{-3}$
A
10
5
0
-5
-10
-15
$\theta_{MRW} \times 10^{-1}$
B
260
280
300
320
Wavelength (nm)

Figure 3

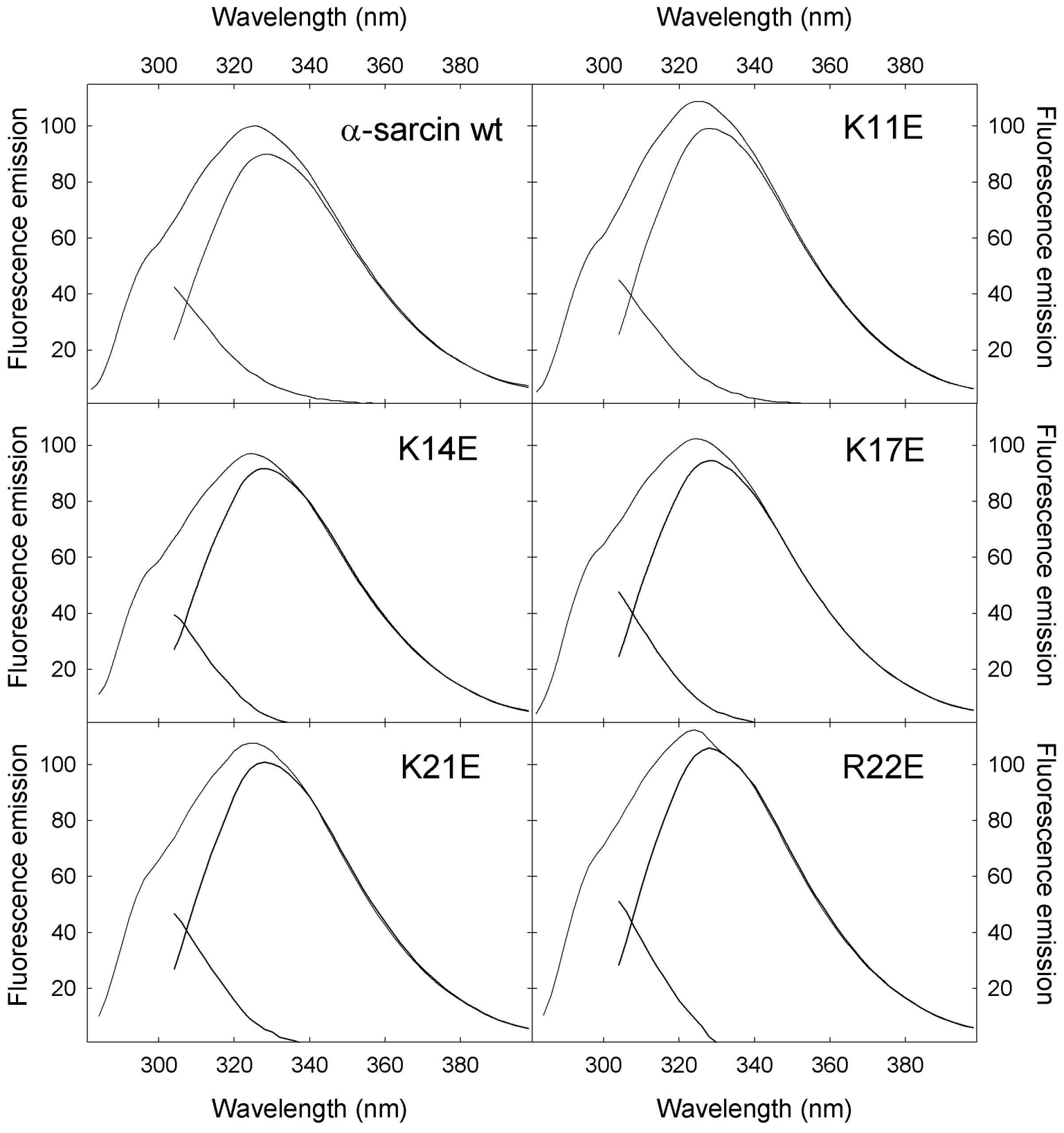
Wavelength (nm)
300
320
340
360
380
Fluorescence emission
20
40
60
80
100
α-sarcin wt
K11E
K14E
K17E
K21E
R22E

Figure 4

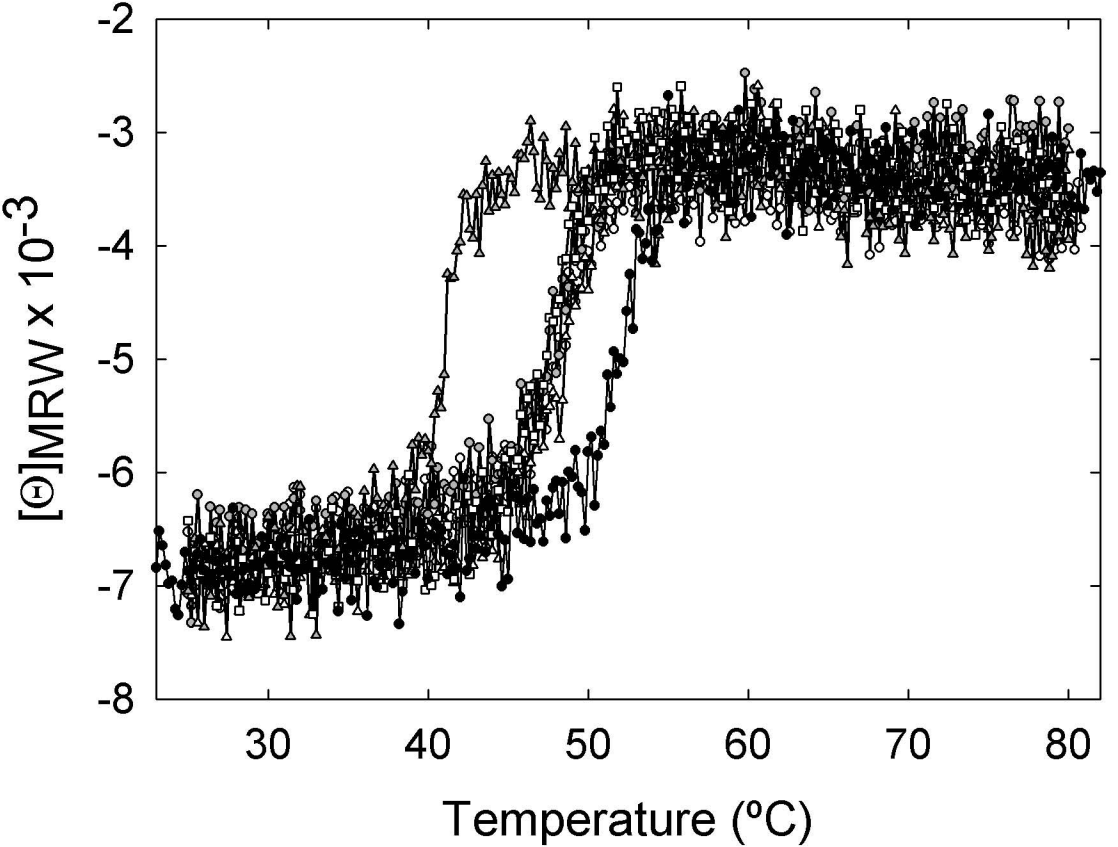

Figure 5

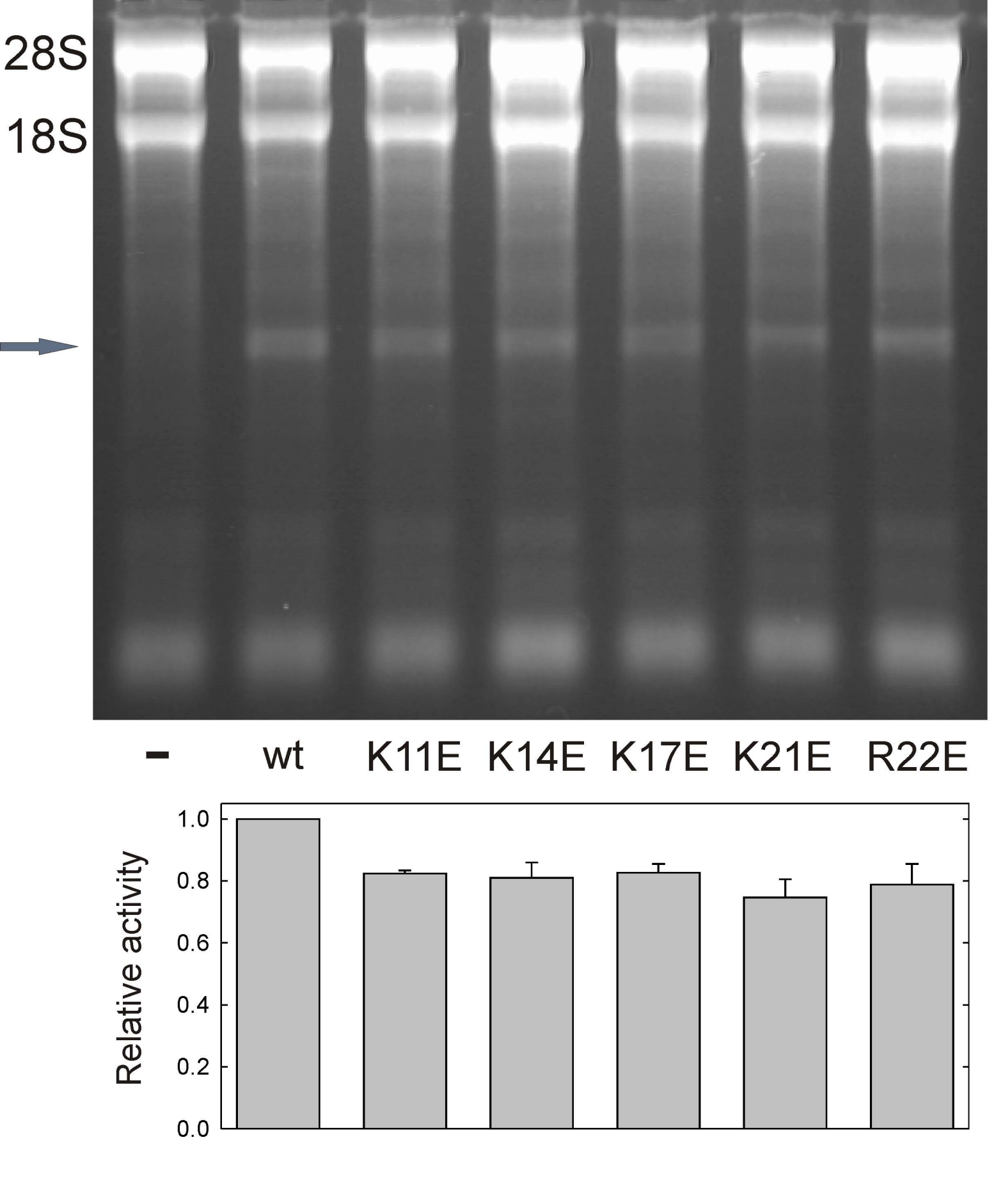
28S
18S
-
wt
K11E
K14E
K17E
K21E
R22E
Relative activity
1.0
0.8
0.6
0.4
0.2
0.0

Figure 6

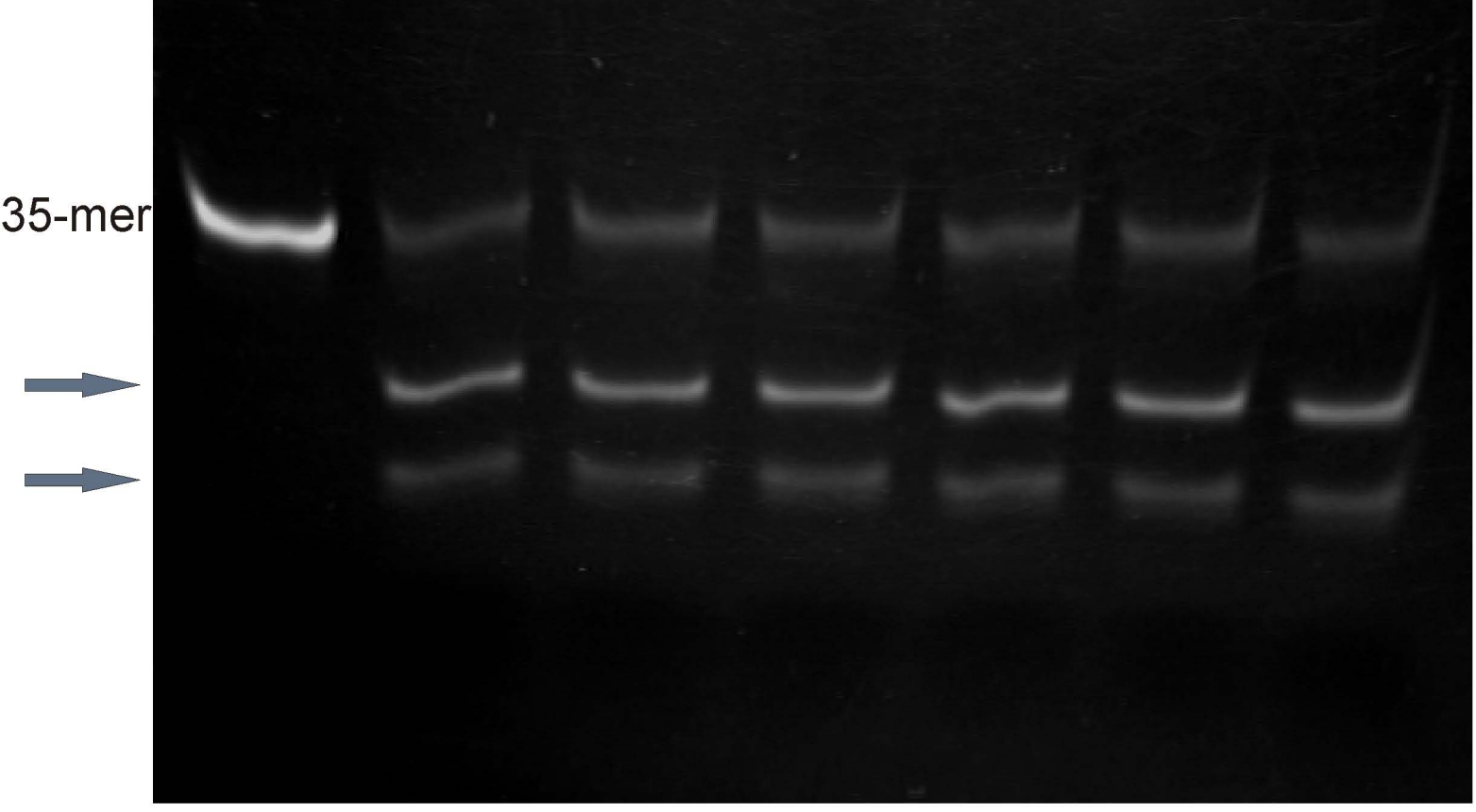
35-mer

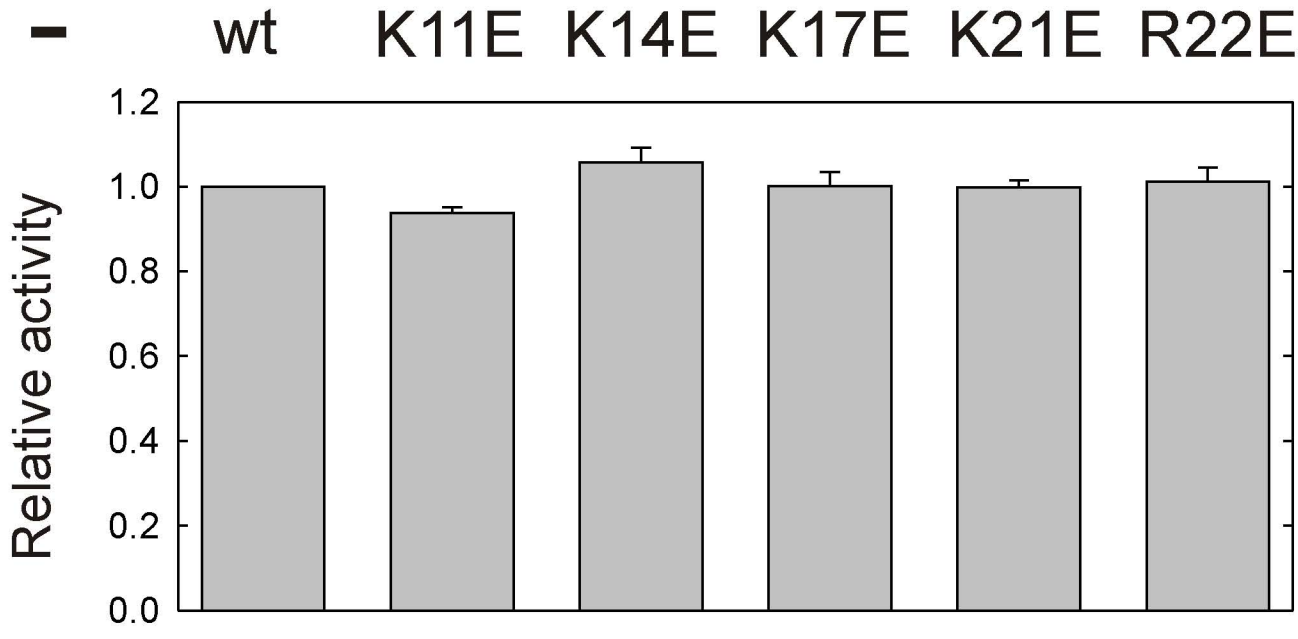
-
wt
K11E
K14E
K17E
K21E
R22E
Relative activity
1.2
1.0
0.8
0.6
0.4
0.2
0.0

Figure 7

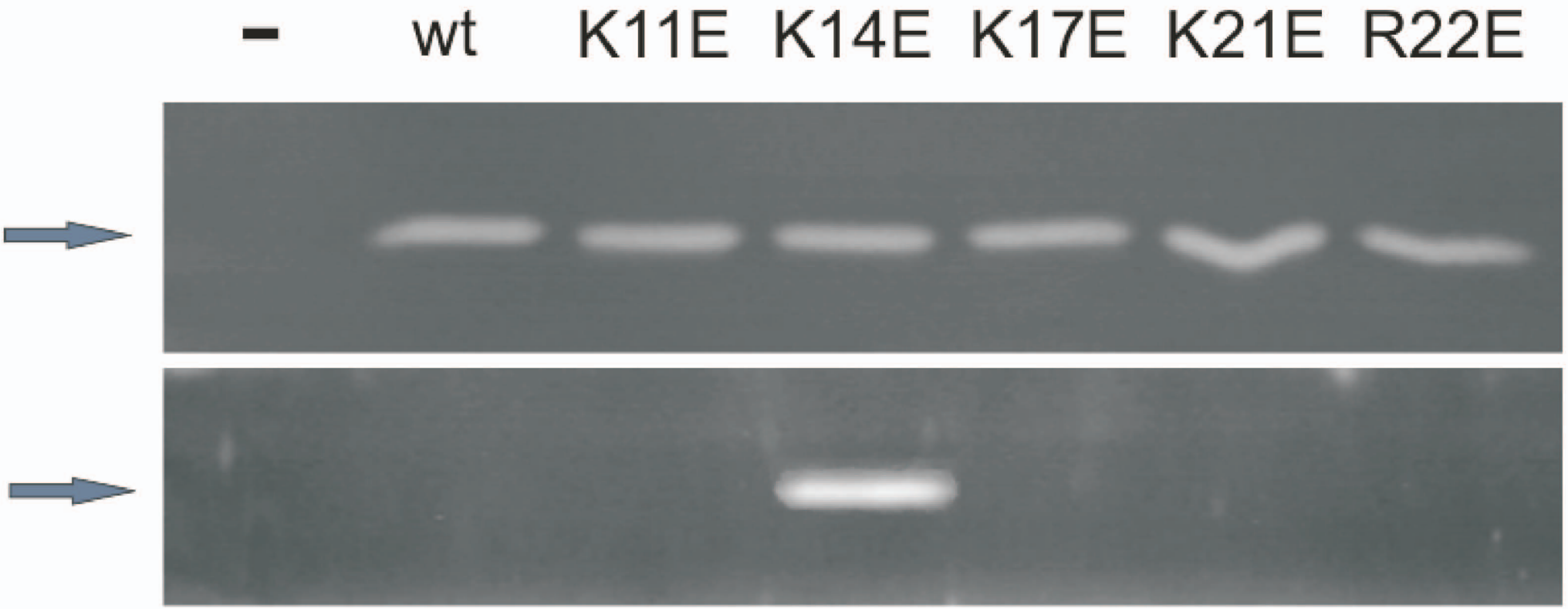

Figure 8

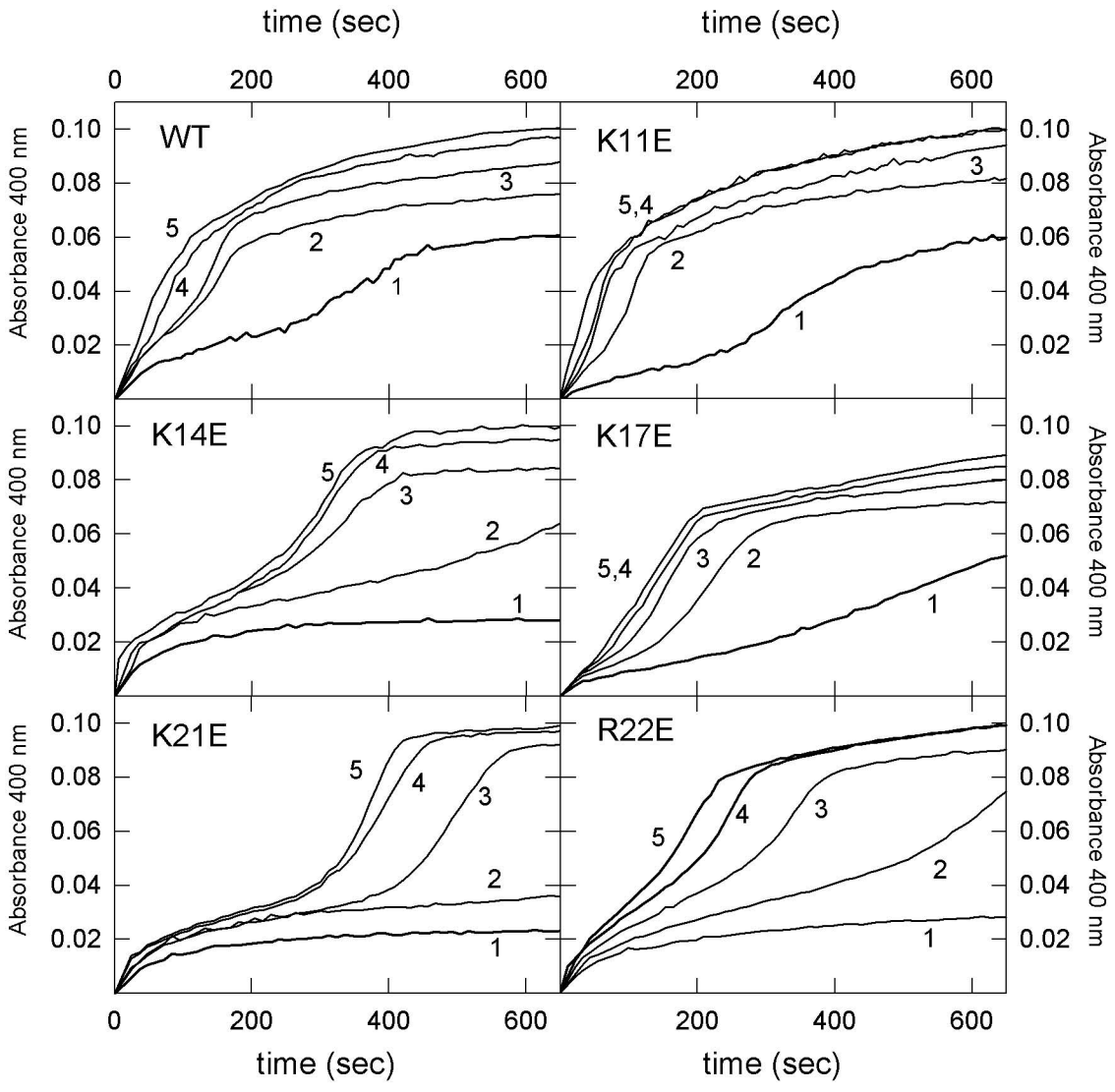
time (sec)
0
200
400
600
WT
K11E
K14E
K17E
K21E
R22E
Absorbance 400 nm
0.10
0.08
0.06
0.04
0.02
1
2
3
4
5
5,4

Figure 9

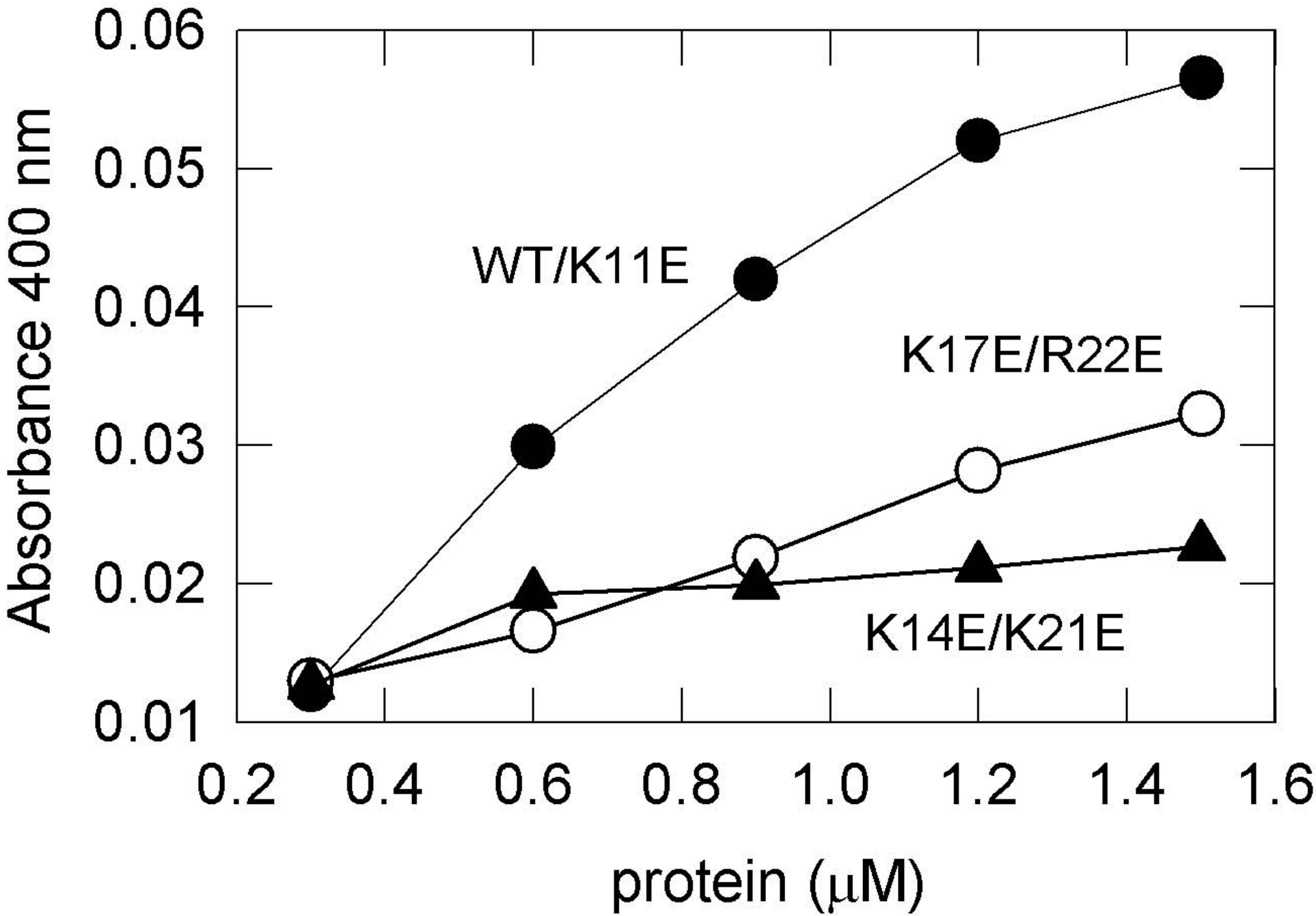
0.06
0.05
0.04
0.03
0.02
0.01
Absorbance 400 nm
WT/K11E
K17E/R22E
K14E/K21E
0.2
0.4
0.6
0.8
1.0
1.2
1.4
1.6
protein (μM)

Figure 10